NJC

Accepted Manuscript

This is an *Accepted Manuscript*, which has been through the Royal Society of Chemistry peer review process and has been accepted for publication.

Accepted Manuscripts are published online shortly after acceptance, before technical editing, formatting and proof reading. Using this free service, authors can make their results available to the community, in citable form, before we publish the edited article. We will replace this *Accepted Manuscript* with the edited and formatted *Advance Article* as soon as it is available.

You can find more information about *Accepted Manuscripts* in the Information for Authors.

Please note that technical editing may introduce minor changes to the text and/or graphics, which may alter content. The journal's standard Terms & Conditions and the Ethical guidelines still apply. In no event shall the Royal Society of Chemistry be held responsible for any errors or omissions in this *Accepted Manuscript* or any consequences arising from the use of any information it contains.

ROYAL SOCIETY OF CHEMISTRY

www.rsc.org/njc

Cite this: DOI: 10.1039/c0xx00000x

www.rsc.org/xxxxxx

ARTICLE TYPE

Diiron hexacarbonyl complexes bearing naphthalene-1,8-dithiolate moiety bridge as the mimics of the sub-unit of [FeFe]-hydrogenase: Synthesis, characterisation and electrochemical investigations

Guifen Qian,[b] Wei Zhong,[a] Zhenhong Wei,[b] Hailong Wang,[a] Zhiyin Xiao,[a] Li Long[a] and Xiaoming Liu*[a, b]

Received (in XXX, XXX) Xth XXXXXXXXX 20XX, Accepted Xth XXXXXXXXX 20XX
DOI: 10.1039/b000000x

Eight diiron hexacarbonyl complexes bearing 1,8-dithionaphthalenyl bridging linkage as the mimics of the diiron subunit of [FeFe]-hydrogenase are reported. Reaction of $Fe_3(CO)_{12}$ with naphtha[1,8-*cd*][1,2]dithiole-n-carbaldehyde (n = 2: **2a** or 4: **2b**) gave two complexes, $[Fe_2(\mu\text{-}S)_2R(CO)_6]$ ($^{-}SRS^{-}$ = n-formylnaphthalene-1,8-bis(thiolate), n = 2: **3a**, 4: **3b**), which were further used as precursors to prepare other six complexes by manipulating the formyl groups. Converting the corresponding formyl group into hydroxymethyl group (CH_2OH) led to complexes **4a** and **4b**. Their reactions with halobutanoyl chloride formed complexes **5a** and **5b** (halo group = Cl), **6a** and **6b** (halo group = Br), respectively. Among the complexes, **3a**, **3b**, **4b**, **5b**, and **6a** were crystallographically analysed. Electrochemical investigations into these complexes revealed that the formyl group exerts profound electronic influence on the electrochemistry and thus catalysis on proton reduction due to its involvement in the conjugation of the bridging linkage. DFT calculations indicate that the formyl group influences the electrochemistry and catalysis by altering significantly the composition of the LUMOs.

1. Introduction

Due to the relevance to hydrogen which may be a favourable potential substituent of fossil fuels in the future, structural revelation of [FeFe]-hydrogenase more than a decade ago has inspired greatly synthetic chemists to mimic the metal centre.[1, 2] In the past decade, a large number of diiron complexes of a core, "$Fe_2(CO)_{6\text{-}X}$" (x = 1 or 2) as the mimics of the diiron subunit (Fig. 1) of the enzyme has been reported.[3-8] Among the reported diiron mimics, some of the models replicate nicely the key features of the diiron subunit of the metalloenzyme, for example, showing a vacant binding site at one of the diiron core,[9] possessing mixed oxidation states for the diiron centre,[10-14] the proton transferring role of the azo-bridging group in hydrogen oxidation and hence reducing overpotential *via* PCET (proton coupled electron transfer) mechanism.[15-18] The azo character has been firmly confirmed recently by incorporating a mimic with the azo linkage into an apo enzyme.[19] Otherwise, the constructed artificial enzyme does not have activity at all. As an electrocatalyst for proton reduction, electrochemical investigations of those mimics have been one of the main concerns in the mimetic chemistry of this enzyme, particularly, the mechanism of election transfer of the diiron mimics.

There is no doubt about the nature of two-electron transfer for the diiron mimics.[5, 6, 20-22] For the electron transfer involving two electrons, the electron transfer process fall into three categories in theory, Scheme 2. If the monoanion is thermodynamically stable enough, normal two sequential one-electron processes (pathway i) are expected with peak potential separation over 400 mV. But so far, there is no precedent example of diiron mimics following this mechanism. Increasing the instability of the monoanion will positively shift the second reduction potential. Therefore, the separation of the two peak potentials will decrease and in an extreme situation become a perfect two-electron process, that is, the two electron processes appears as one single reduction wave. This can be defined as **EE** process (pathway ii). Such a classic example is the oxidation of Zn into Zn^{2+}.[23] For diiron mimics, due to the instability of the monoanion, a chemical reaction is followed, which is an isomerisation, likely decoordinating one of the four Fe(I)–S bonds to lower the electron density on the dimetal centre.[24, 25] The coupled reaction generates such a species that its reduction occurs at a potential not more negative than the first one. This is generally called potential inversion, that is, the so-called **ECE** process.[5, 6, 20, 21] When the coupled reaction is extremely fast, a perfect two-electron process is expected (pathway ii). A typical example is the diiron complex derived from 1,2-dithiobenzene and its derivatives.[22, 26-29]

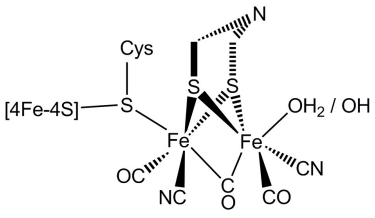

Fig. 1 Schematic view of the H-cluster of [FeFe]-hydrogenase.

Recently, we investigated, in detail, the electrochemistry of diiron hexacarbonyl complex bearing a bridging linkage of (1,8-dithionaphthalen-2-yl)methyl ferrocenylcarboxylate and found that the complex adopts essentially the mechanism iii shown in Scheme 1 and further found by DFT calculations that the dianion ($[Fe_2]^{2-}$) generated from the two sequential one-electron transfer isomerises to the other dianion ($[Fe_2]'^{2-}$) resulting from the **ECE** processes.[30] The species $[Fe_2]'^{2-}$ is supposedly more stable by decoordinating one of four Fe–S bonds to lower the electron density on the diiron centre. In other word, for this complex, the two pathways co-exist to compete with each other. Such a mechanism was also found in other systems without conjugation like the naphthalene and benzene.[31, 32] In the two competing processes, which one will prevail is mainly dictated by the nature of the bridging linkage and thus the thermodynamic stability of the monoanion right after accepting the first electron. Interestingly, the mechanism seems to apply to diiron complexes of various oxidation states.[33]

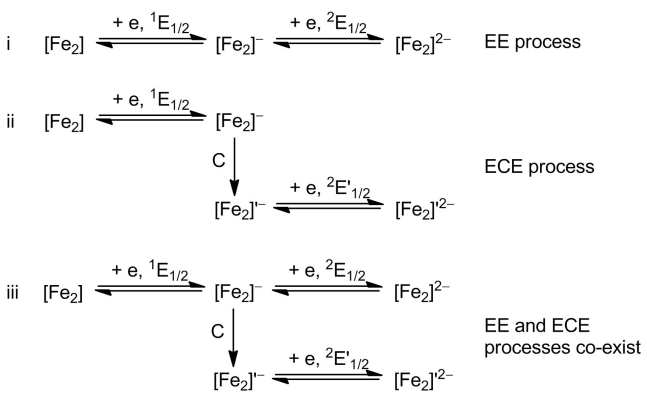

Scheme 1 The pathways of electron transfer involved in the reduction of diiron mimics of [FeFe]-hydrogenase. Please note that (a) pathway iii is the combination of i and ii, (b) $[Fe_2]$ refers to the diiron mimics.

Ideally, a mimic should exhibit robustness upon reduction for decent catalytic performance in catalysing proton reduction. However, among the numerous mimics reported in the literatures,[3-8] most of the diiron complexes exhibit an irreversible reduction. Since the diiron mimics with the naphthalenyl bridging linkage is one of the limited systems showing reversibility upon reduction,[34-39] we are interested in exploring the positions 2 and 4 on the aromatic system for diiron mimics bearing a variety of substituents. The substituents on these positions exert both steric and electronic not only on the bridging linkage, but also provide possibilities for further functionalising the mimics. Herein, we report the synthesis, characterisation, electrochemical investigation of eight diiron hexacarbonyl complexes (**3a**, **3b**, **4a**, **4b**, **5a**, **5b**, **6a** and **6b**) to be supplementary to our work reported recently.[30] These complexes were fully characterised using a variety of techniques (FTIR, NMR, Elemental analysis). The structures of most of these complexes (**3a**, **3b**, **4b**, **5b** and **6a**) were determined using X-ray single crystal diffraction analysis. Electrochemistry of these diiron complexes as well as the naphthalenyl compounds containing formyl group (**2a** and **2b**) was investigated. It was found that the influence on the electrochemistry and the catalysis of these mimics on proton reduction exerted by the substituents on the naphthalene ring depended mainly on whether the conjugation of the naphthalene cycles is disturbed or not. But the formyl group showed the most profound influence compared with other substituents due to its taking part in the conjugation. To probe the molecular mechanism of its effect, DFT calculations for complexes **3a**, **3b**, **4a** and **4b** were also performed.

2. Experimental

2.1 General procedures

All solvents were distilled prior to use and stored under an argon atmosphere. Unless otherwise stated, all syntheses and manipulations were performed using Schlenk technique. $NaBH_4$, 4-halobutanoyl chloride (4-$Cl(CH_2)_3COCl$ and 4-$Br(CH_2)_3COCl$) were purchased from either Alfa Aesar or Sigma-Aldrich and used as received. $Fe_3(CO)_{12}$[40] and ferrocenecarbonyl chloride (FcCOCl)[41] were synthesised following the literature processes. Naphtho[1,8-*cd*][1,2]dithiole (**1**) and naphtha[1,8-*cd*][1,2]dithiole-n-carbaldehyde (n = 2: **2a** and n = 4: **2b**) were synthesised as described in the literature.[42]

FTIR spectra were recorded on Scimitar 2000 (Varian). NMR spectra were collected on Avance DRX 400 (Varian) in $CDCl_3$. Element analysis was carried out on Vario ELIII elemental analyzer. X-ray diffraction data were collected on Siemens SMART System CCD at room temperature. Electrochemistry was performed in 0.5 mol L^{-1} $[Nbu_4]BF_4$-CH_2Cl_2 or 0.1 mol L^{-1} $[Nbu_4]BF_4$-MeCN by using vitreous carbon disc (ϕ = 1 mm) as working electrode, vitreous carbon strip as counter electrode and Ag / AgCl against which the potential of ferrocenium / ferrocene couple is 0.55 V.[43, 44] A scanning rate of 0.1 Vs^{-1} was routinely used unless otherwise stated. All potentials were quoted against a ferrocenium / ferrocene couple.

2.2 Crystallographic data collection

Crystals suitable for X-ray analysis were obtained by the slow evaporation of a solution in hexane / dichloromethane. Diffraction data were collected on a Bruker SMART CCD diffractometer with graphite-monochromated Mo–Kα radiation (λ = 0.71073 Å). The crystal structures were solved using direct methods in SHELXS program and refined by full-matrix least-squares routines, based on F^2, using the SHELXL package.[45] CCDC 895027–895029 and 895031–895033 for the complexes **3a**, **3b**, **4b**, **5b**, **6a** and **7** contain the supplementary crystallographic data for this paper. These data can be obtained free of charge from The Cambridge Crystallographic Data Centre *via* www.ccdc.cam.ac.uk/data_request/cif.

2.3 DFT calculations

All calculations were carried out by using Gaussian 03 package.[46] DFT calculations were carried out using the BP86 functional[47, 48] and a valence triple-ζ basis set with polarization on all atoms (TZVP).[49] Geometry optimizations of the investigated complexes were performed without any symmetry constraints in the ground state, the initial geometries are derived from the crystallographic data. Frequency calculations were carried out to ensure that the obtained geometries are at a minimum on the potential energy surface with no imaginary frequencies. Based on the optimized geometries, the orbital energies and compositions of the HOMOs

and LUMOs of the studied complexes were calculated.

2.4 Synthesis

2.4.1 Preparation of $[Fe_2((\mu\text{-}S)_2C_{10}H_5\text{-}n\text{-}CHO)(CO)_6]$ (n = 2: 3a, 4: 3b). A mixture of **2a** (130 mg, 0.596 mmol) and $[Fe_3(CO)_{12}]$ (331 mg, 0.656 mmol) in toluene (25 mL) was refluxed at 110 °C for 1.5 h. The reaction was allowed to cool to room temperature before filtration was carried out to remove any insoluble solids. The filtrate was concentrated under reduced pressure. Before being purified using flash column chromatography (silica gel, eluents: petroleum ether / DCM = 2 / 3). The product was collected as a dark-red powder (178 mg, 60%). Recrystallisation was performed in a mixture of DCM and hexanes at –20 °C to give single crystals suitable for X-ray diffraction analysis. Infrared spectral absorption bands for complex **3a** (DCM, cm^{-1}): ν (CO), 2078.4, 2043.6, 2004.4, (KBr) ν (CHO), 1690.6. ^1H NMR ($CDCl_3$, ppm): δ 11.29 (1H, s, C*H*O), 8.23 (1H, d, J = 6.8 Hz, *Naph*), 7.95 (3H, d, J = 5.2 Hz, *Naph*), 7.44 (1H, t, J = 7.6Hz, *Naph*). ^{13}C NMR ($CDCl_3$, ppm): 207.27, 191.40, 133.86, 132.41, 131.47, 127.81, 127.23, 123.97. Microanalysis for complex **3a** ($C_{17}H_6Fe_2O_7S_2$, MW = 498.05), calc. (found): C%, 41.00 (40.33), H%, 1.21 (1.37). The relatively large discrepancy between the calculated and the determined values may result from involvement of moisture during the operation. Since addition of 0.46 equivalent of H_2O to the complex gave decent result, calc. (found): C%, 40.33 (40.33), H%, 1.38 (1.39).

3b was analogously prepared as a dark red solid (202 mg, 68%). Infrared spectral bands for complex **3b** (DCM, cm^{-1}): ν (CO), 2077.5, 2042.5, 2003.3, (KBr) ν (CHO), 1689.7. ^1H NMR ($CDCl_3$, ppm): δ 10.29 (1H, s, C*H*O), 9.39 (1H, d, J = 8.4 Hz, *Naph*), 8.37 (1H, d, J = 7.6 Hz, *Naph*), 8.22 (1H, d, J = 7.6 Hz, *Naph*), 7.81 (1H, d, J = 7.6 Hz, *Naph*), 7.50 (1H, t, J = 7.8 Hz, *Naph*). Micro-analysis for **3b** ($C_{17}H_6Fe_2O_7S_2$, MW = 498.05), calc. (found): C%, 41.00 (40.37), H%, 1.21 (1.38).

2.4.2 Preparation of $[Fe_2((\mu\text{-}S)_2C_{10}H_5\text{-}n\text{-}CH_2OH)(CO)_6]$ (n = 2: 4a, 4: 4b). To a solution of **3a** (148 mg, 0.297 mmol) in dry THF (30 mL) was added $NaBH_4$ (10 mg, 0.266 mmol) at ice temperature. The reaction mixture was stirred for about 2 h under Ar. After the completion of the reaction (monitored by TLC), the solution was evaporated under reduced pressure to give crude product. Purification on a silica-gel column using a mixture of dichloromethane / petroleum ether (3 / 2) as eluent to produce a dark red solid (**4a**,100 mg, 67%). The crude product was recrystallised in hexane-dichloromethane. Infrared spectral bands for complex **4a** (DCM, cm^{-1}): ν (CO), 2075.4, 2040.2, 2000.2, (KBr) ν (OH), 3437.6. ^1H NMR ($CDCl_3$, ppm): δ 8.26 (1H, d, J = 8.4 Hz, *Naph*), 8.00 (2H, m, *Naph*), 7.74 (1H, d, J = 8.4 Hz, *Naph*), 7.39 (1H, t, J = 7.8 Hz, *Naph*), 5.32 (2H, d, *J* = 6.4 Hz, CH_2), 2.15 (1H, t, J = 6.2 Hz, O*H*). ^{13}C NMR ($CDCl_3$, ppm):144.07, 135.89, 133.74, 133.18, 132.28, 131.42, 125.85, 125.05, 64.31. Micro-analysis for **4a** ($C_{17}H_8Fe_2O_7S_2$, MW = 500.06), calc. (found): C%, 40.83 (40.51), H%, 1.61 (1.69).

4b was analogously prepared as a dark red solid (101 mg, 68%). Infrared spectral bands for complex **4b** (DCM, cm^{-1}): ν(CO), 2074.9, 2039.3, 1999.5. ^1H NMR ($CDCl_3$, ppm): δ 8.32 (1H, d, J = 8.4 Hz, *Naph*), 8.27 (1H, d, J = 7.6 Hz, *Naph*), 8.23 (1H, d, J = 7.6 Hz, *Naph*), 7.47 (2H, m, *Naph*), 5.14 (2H, d, J = 5.6 Hz, CH_2), 1.88 (1H, t, J = 5.8 Hz, O*H*). ^{13}C NMR ($CDCl_3$, ppm): 207.63, 140.26, 132.79, 132.46, 132.38, 127.40, 126.96, 125.80, 125.60, 125.00, 124.62, 63.56. Micro-analysis for **4b** ($C_{17}H_8Fe_2O_7S_2$, MW = 500.06), calc. (found): C%, 40.83 (40.67), H%, 1.61 (1.56).

2.4.3 Preparation of $[Fe_2((\mu\text{-}S)_2C_{10}H_5\text{-}n\text{-}CH_2O_2C(CH_2)_3Cl)(CO)_6]$ (n = 2: 5a, 4: 5b). To a solution of **4a** (32 mg, 0.064 mmol) in DCM (10 mL) was added Et_3N (0.01 mL) and 4-chlorobutanoylchloride (0.008 mL, 0.071 mmol), respectively, at ice temperature. The reaction mixture was stirred for 30 min under Ar. When the reaction was completed (monitored by TLC), the solvent was evaporated under reduced pressure. Purification on a silica column using dichloromethane / petroleum ether (1:1) as eluent gave a dark red solid (**5a**, 35 mg, 91%). Infrared spectral bands for complex **5a** (DCM, cm^{-1}): ν (CO), 2075.8, 2040.6, 2000.8. ^1H NMR ($CDCl_3$, ppm): δ 8.27 (1H, d, J = 7.2 Hz, *Naph*), 7.99 (2H, m, *Naph*), 7.58 (1H, d, J = 8.4 Hz, *Naph*), 7.41 (1H, m, *Naph*), 5.75 (2H, s, PhCH_2O), 3.64 (2H, t, J = 6.2 Hz, ClCH_2), 2.65 (2H, t, J = 7.4 Hz, COCH_2), 2.17 (2H, m, $CH_2CH_2CH_2$). ^{13}C NMR ($CDCl_3$, ppm): 207.43, 172.27, 138.83, 134.02, 133.28, 132.21, 131.24, 127.15, 126.79, 125.50, 125.01, 124.37, 65.51, 44.04, 31.13, 27.58. Micro-analysis for **5a** ($C_{21}H_{13}ClFe_2O_8S_2$, MW = 604.60), calc. (found): C%, 41.72 (41.33), H%, 2.17 (2.07).

5b (dark-red solid, 33 mg, 85%) was analogously prepared as **5a**. Infrared spectral absorption bands for complex **5b** (DCM, cm^{-1}): ν (CO), 2075.4, 2040.2, 2000.2. ^1H NMR ($CDCl_3$, ppm): δ 8.28 (1H, d, J = 7.6 Hz, *Naph*), 8.21 (2H, m, *Naph*), 7.48 (2H, t, J = 6.6 Hz, *Naph*), 5.55 (2H, s, PhCH_2O), 3.58 (2H, t, J = 6.2 Hz, ClCH_2), 2.59 (2H, t, J = 7.0 Hz, COCH_2), 2.12 (2H, m, $CH_2CH_2CH_2$). Micro-analysis for **5b** ($C_{21}H_{13}ClFe_2O_8S_2$, MW = 604.60), calc. (found): C%, 41.72 (41.78), H%, 2.17 (2.28).

2.4.4 Preparation of $[Fe_2((\mu\text{-}S)_2C_{10}H_5\text{-}n\text{-}CH_2O_2C(CH_2)_3Br)(CO)_6]$ (n = 2: 6a, 4: 6b). 6a and **6b** were produced in the same manner as that for **5a** and **5b** by using **4a** and **4b** (408 mg, 0.816 mmol) to produce **6a** (433 mg, 95%) and **6b** (527 mg, 99%) respectively. Infrared spectral bands for complex **6a** (DCM, cm^{-1}): ν (CO), 2075.9, 2040.6, 2001.0. ^1H NMR ($CDCl_3$, ppm): δ 8.27 (1H, d, J = 7.6 Hz, *Naph*) , 7.99 (2H, m, *Naph*),7.57 (1H, d, J = 8.4 Hz, *Naph*), 7.41 (1H, t, J = 7.8 Hz, *Naph*), 5.75 (2H, s, PhCH_2O), 3.50 (2H, t, J = 6.4 Hz, ClCH_2), 20.65 (2H, t, J = 7.2 Hz, COCH_2), 2.26 (2H, m, $CH_2CH_2CH_2$). ^{13}C NMR ($CDCl_3$, ppm): δ 207.34, 172.06, 138.81, 134.00, 133.23, 132.16, 131.18, 127.14, 126.75, 125.46, 125.02, 124.37, 65.47, 32.56, 32.37, 27.67. Micro-analysis for **6a** ($C_{21}H_{13}BrFe_2O_8S_2$, MW = 649.05), calc. (found): C%, 38.86 (38.56), H%, 2.02 (2.02). Infrared spectral bands for complex **6b** (DCM, cm^{-1}): ν (CO), 2075.0, 2039.9, 1999.8. ^1H NMR ($CDCl_3$, ppm): δ 8.235 (3H, m, *Naph*), 7.470 (2H, d, J = 7.2 Hz, *Naph*), 5.545 (2H, s, PhCH_2O), 3.447 (2H, t, J = 6.0 Hz, ClCH_2), 2.591 (2H, t, J = 7.0 Hz, COCH_2), 2.195 (2H, t, J = 4.4 Hz, $CH_2CH_2CH_2$). ^{13}C NMR ($CDCl_3$, 400 MHz): δ 207.41, 172.24, 135.28, 132.88, 132.61, 132.27, 127.20, 126.99, 126.58, 126.16, 126.02, 125.88, 64.28, 32.60, 32.36, 27.52. Micro-analysis for **6b** ($C_{21}H_{13}BrFe_2O_8S_2$, MW = 649.05), calc. (found): C%, 38.86 (39.01), H%, 2.02 (2.11).

2.4.5 Preparation of $[Fe_2(\mu\text{-}S)_2C_{10}H_6(CO)_6]$ (8). Complex **8** (a dark red solid, 246 mg, 87%) was prepared in the same manner as for complex **3a**. Infrared spectral bands for complex **8** (DCM, cm^{-1}): ν (CO), 2074.6, 2038.9, 1999.1. ^1H NMR ($CDCl_3$, ppm): δ

8.26 (2H, d, J = 8.0 Hz, *Naph*), 8.01 (2H, d, J = 8.0 Hz, *Naph*), 7.42 (2H, t, J = 8.0 Hz, *Naph*). ^{13}C NMR ($CDCl_3$, ppm): δ 207.62, 134.30, 132.79, 132.03, 126.55, 125.38, 124.93.

3. Results and discussion

3.1 Synthesis and characterization

Naphtho[1,8-*cd*][1,2]dithiole (**1**) was prepared by following literature procedure.[50] Its derivatives, naphthalene-1,8-disulfide-2-carboxaldehyde (**2a**) and naphthalene-1,8-disulfide-4-carboxaldehyde (**2b**) were prepared using modified literature procedures.[42] Reaction of these disulfides with triiron dodecacarbonyl led to two diiron complexes **3a** and **3b**, respectively. The diiron core of the complexes is robust enough to allow performing reaction on the formyl group without affecting the integrity of the diiron hexacarbonyl core. Reduction of the formyl group by $NaBH_4$ formed complexes **4a** and **4b** by converting the formyl group into hydroxymethyl group. The hydroxyl group could react further with 4-halobutanoyl chloride to form complexes **5a**, **5b**, **6a** and **6b**. In addition to the above diiron carbonyl complexes, complex **8** bearing no substituent on the naphthalene ring was also synthesised by reacting straightway compound **1** with $Fe_3(CO)_{12}$ rather than using its reduced form, naphthalene-1,8-dithiol.[34]

These diiron complexes exhibited characteristic infrared absorption bands of diiron hexacarbonyl complexes, three absorption bands of the bound CO ranging from 2080 to 2000 cm^{-1}, Fig. S1. All the infrared data are tabulated in Table 1. For comparison, the infrared absorption bands of the complex (**8**) derived from naphtho[1,8-*cd*][1,2]dithiole was also included. The data fall into two categories. For **3a** and **3b**, all the absorption bands are at higher frequencies by a few wavenumbers. This shift is attributed to the nature of electron-withdrawing of the formyl group and its conjugation with the naphthalene ring. For the other complexes, although the substituents on the aromatic ring vary, these groups have electronically little influence on the absorption bands. The UV-vis spectra of complex **3a** and **3b** showed similar characteristic feature as found in their infrared spectra, Fig. S2.

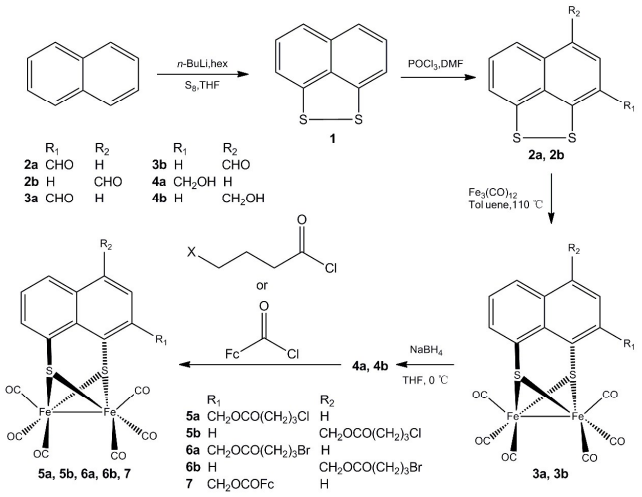

Scheme 2 Synthesis of the naphthalene derivatives and the eight diiron complexes and 7.[30]

Table 1 FTIR absorption bands (CO) for diiron hexacarbonyl complexes in DCM.

Complex	ν_{CO} / cm^{-1}
[a]**3a**	2078.4, 2043.6, 2004.4, [b]1690.6
[a]**3b**	2077.5, 2042.5, 2003.3, [b]1689.7
4a	2075.4, 2040.2, 2000.2
4b	2074.9, 2039.3, 1999.5
5a	2075.8, 2040.6, 2000.8, [b]1738.3
5b	2075.4, 2040.2, 2000.2, [b]1740.6
6a	2075.9, 2040.6, 2001.0, [b]1737.6
6b	2075.0, 2039.9, 1999.8, [b]1739.9
[c]**7**	2075.0, 2039.9, 2000.1, [b]1723.3
8	2074.6, 2038.9, 1999.1

[a]The absorption bands of the formyl group of **2a** and **2b** are 1642.6 and 1664.1 cm^{-1} (KBr), respectively.
[b]Organic carbonyl group (KBr).
[c]Quoted from reference 30.

3.2 Structural analysis

The molecular structures of diiron hexacarbonyl complexes **3a**, **3b**, **4b**, **5b** and **6a** were confirmed by X-ray analysis. It should be noted that the molecular structure of complex **7** was also determined by X-ray crystallography even though other characterizations of this complex had been reported in our recent work.[30] Crystal structures are shown in Fig. 2 and crystallographic details and selected binding parameters are listed in Table 2 and Table 3, respectively. In the case of complex **7**, the structure includes a molecule of dichloromethane solvent, with a polymorph not including the solvent given in Fig. 2. All of the crystal structures possess a $[Fe_2S_2]$ butterfly core and in which the two iron centres are linked to three carbonyl ligands in a distorted square-pyramidal geometry, as previously reported in the analogous complexes.[34, 35, 51] As indicated by the data in Table 3, the Fe−Fe bond length (2.50~2.53 Å) as well as the Fe−S bond length between each iron and each sulphur (2.23~2.25 Å) for these complexes are comparable with each other. Together with some representative bond angles shown in Table 3, those parameters are not altered very much with the different substituent or different position on the naphthalene moiety.

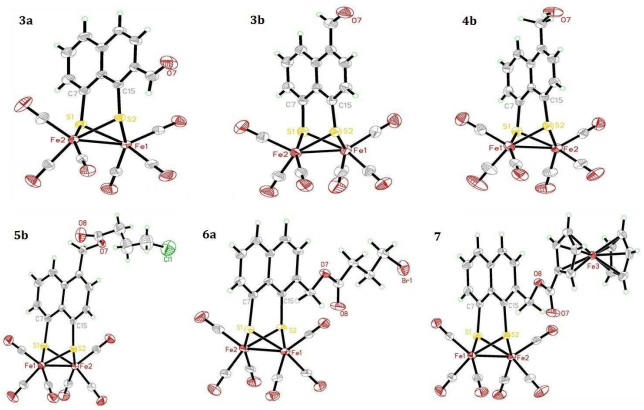

Fig. 2 Structural views of complexes **3a**, **3b**, **4b**, **5b**, **6a** and **7**.

3.3 Electrochemistry

All the diiron complexes exhibited at least two reduction and one oxidation processes, Table 4, Fig. 3 and Fig. S3. For reference, the electrochemistry of compounds **2a** and **2b** are also shown in Fig. S4. Further scanning towards negative potential could reveal more reduction process which may be assigned to a dimer generated from the reaction of the dianion and its parent complex.[22]

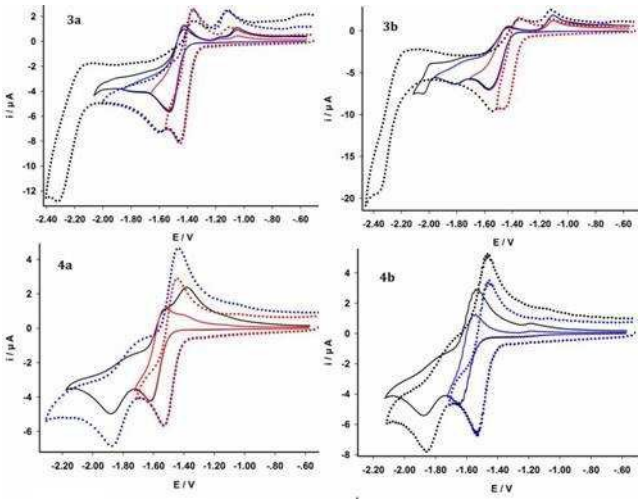

Fig. 3 Cyclic voltammograms (CVs) of complexes **3a**, **3b**, **4a** and **4b** (C = 2.86 mmol L^{-1}) on vitreous carbon electrode in 0.1 mol L^{-1} $[NBu_4]BF_4$ / CH_3CN (dot line) or 0.5 mol L^{-1} $[NBu_4]BF_4$ / DCM (solid line) solution at a scan rate of 0.1 Vs^{-1} (298 K, *vs*/Fc+). Blue or red colour is used to distinguish the CVs obtained within various ranges of scanning potentials.

Our previous investigation into complex **7** suggested that the electron transfer of the complex comprises two competing pathways with potential inversion (pathway iii, Scheme 1).[30] As suggested by their electrochemistry, responses to the variation in scanning rates and current functions (Figs. 3, S3, S5 and S6), these complexes except for complexes **3a** and **3b** would adopt similar mechanisms for their charge transfer. The separation of the two reductions of these complexes is sensitive to solvents. The gap between the two processes is widened in polar solvent, such as acetonitrile and DMF, compared with nonpolar solvent (DCM). This indicates that in polar medium, the monoanion is somewhat stabilised and alter the energies of the LUMOs. This can be attributed to electrostatic and hydrogen bonding interactions between the monoanion and the solvents. Such an interaction is in agreement with what we found recently that intramolecular interaction exerts electronic influence on the frontier orbitals.[52]

Among the complexes, complexes **3a** and **3b** show distinct feature in their reductions from the other complexes. This is particularly obvious in DCM. In this medium, the two reductions are almost indistinguishable except for slight broadening of the wave. Increasing scanning rate enhances the second reduction which becomes visible as shown in Fig. S4. This indicates that the formyl group exerts much stronger electronic influence on the diiron centre compared with other substituents. As shown in their structures, the formyl group at either position (2 and 4) adopts a coplanar orientation with the naphthalene moiety (Fig. 1) and the conjugation between the aromatic ring and the formyl group is established. This conjugation may be the root-cause of the profound difference in their reductions as formyl group is of electron-withdrawing nature. This means that expanding the conjugation with the naphthalene rings ought to be beneficial to lowering the electron density on the metal centre and therefore, stabilising the monoanion. In other word, larger potential separation for the two processes would be expected. But the observation is on the contrary. By considering that the aldehydes of the bridging linkages show reduction processes between −1.5 and −1.8 V (Fig. S4), the observed reduction processes may contain both metal-based and ligand-based processes.

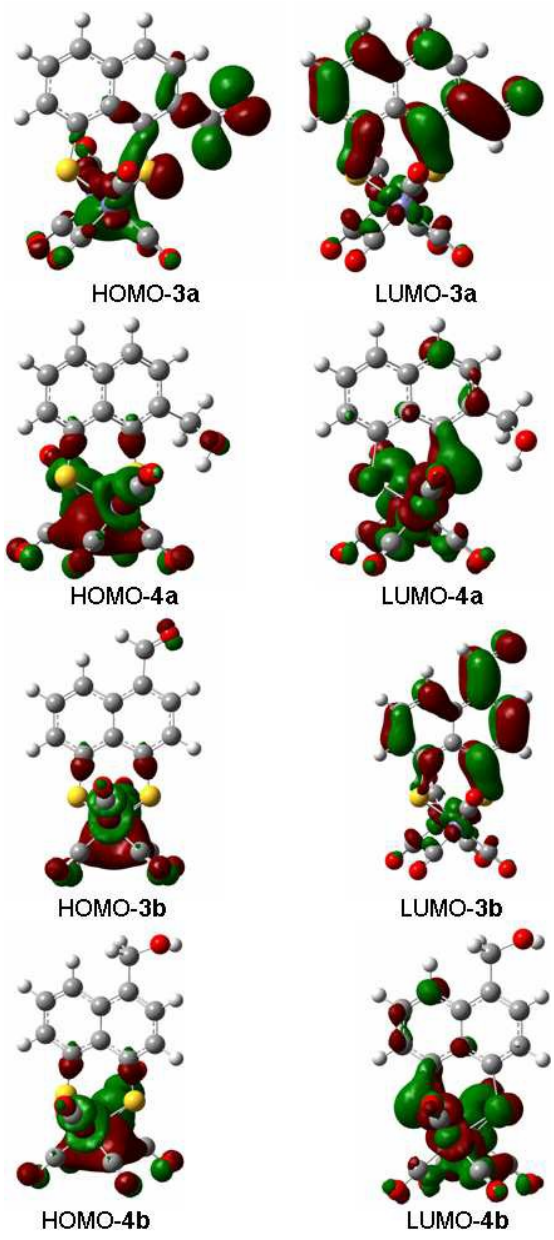

Fig. 4 The HOMOs and LUMOs of complexes **3a**, **3b**, **4a** and **4b**.

Table 5 The energies and compositions of the HOMOs and LUMOs of complexes **3a** and **3b**, **4a** and **4b**.

Complex	E_{HOMO}	E_{LUMO}	HOMO		LUMO	
			Bridging linkage	{Fe_2}	Bridging linkage	{Fe_2}
3a	-6.16007	-3.97729	72.4%	27.6%	67.5%	32.5%
3b	-6.24116	-4.0649	43.6%	56.4%	67.8%	32.2%
4a	-6.14728	-3.68668	43.3%	56.7%	12.8%	87.2%
4b	-6.04171	-3.55689	42.7%	57.3%	9.8%	90.2%

To support this argument, complexes **3a** and **3b**, **4a** and **4b** were chosen for theoretical calculations and the energies and compositions of their HOMOs and LUMOs were calculated. Recently, we used DFT calculations to examine how a bridging linkage affects the compositions of the HOMOs and LUMOs of a diiron hexacarbonyl mimics.[52] It was found that the linkage has significant influence on the compositions of the HOMOs, and the LUMOs were mainly located on the diiron centre in all the examples examined. But the calculations (Table 5, Fig. 4) for the four complexes showed that there are significant differences between the complexes. The results for complexes **4a** and **4b** follow the suit well that their LUMOs were mainly located on the diiron centre, but the LUMOs of complexes **3a** and **3b** are mostly dominated by the organic motif by about two third (Fig. 4 and Table 5). The orbital compositions suggest that the first reductions of the two complexes (**3a** and **3b**) are very much dominated by the bridging linkages. The involvement of the bridging linkage in their LUMOs may explain why the two complexes with formyl group behave rather differently from the others in their reduction processes (Figs. 3 and S3).

3.4 Catalysis on the reduction of proton

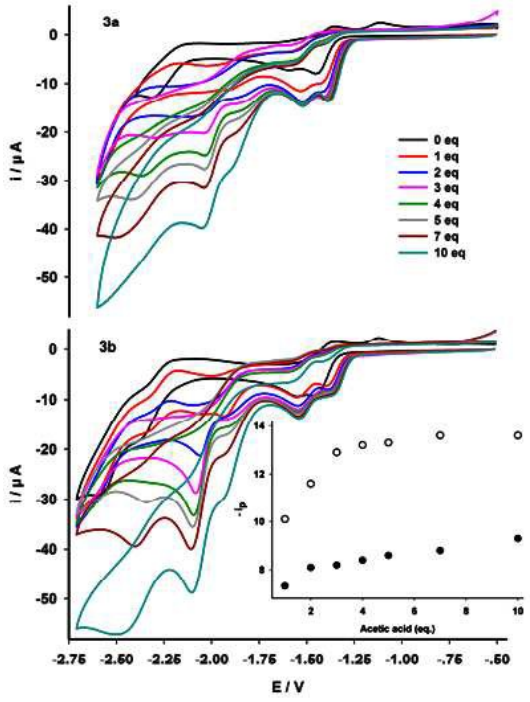

Fig. 5 The cyclic voltammograms of complexes **3a** and **3b** (C = 2.86 mmol L^{-1}) in acetic medium-acetonitrile (inset: the plot of catalytic current of the first reduction peak against the concentration of acetic acid for **3a** (circle) and **3b** (solid), respectively. The potentials were quoted against Fc/Fc^+ couple).

Catalysis on proton reduction by these complexes was examined in DCM and / or acetonitrile by using acetic acid as proton source, Figs. 5 and S7. The results revealed that all the complexes showed no sign of catalysis at the first reduction process except complexes **3a** and **3b**. And significant increases in currents were observed at far negative potential, which is attributed to the catalysis of the diiron mimics (Fig. S8). This observation suggests among the co-existing and competing EE and ECE mechanisms we reported recently,[30] the EE mechanism prevails. It means that in the first reduction, the dianion generated from the ECE process and with strong affinity towards proton is not dominant. What is surprising is that complexes **3a** and **3b** showed catalysis on proton reduction to some extent. As shown in Table 4, the reduction potentials of the two complexes are the most positive ones among the complexes, which indicate relatively lower electron density on the metal centre compared with the other complexes. These observations are in good agreement with their blue shift in infrared absorption bands (Table 1). Apparently, the involvement of the formyl group in the conjugation played a role in reducing electron density on the diiron centre. Since catalytic reduction of proton involves protonation, a catalyst of high electron density must be beneficial to the catalysis. Apparently, the observed catalytic responses of the first reduction of these complexes towards proton reduction are not in agreement with the above argument. This abnormal behaviour may be due to the dominant involvement of the organic moiety in the reduction. Furthermore, the potential of the catalytic process shifts positively over 100 mV (Fig. 5). This positive shift could be caused by proton-coupled electron transfer (PCET) since the reduction of the formyl group ought to involve proton rtansfer. The electrochemistry and catalytic responses towards proton reduction support further the argument that the bridging linkage exerts profound influence on the metal centre of a diiron carbonyl complex.[32] Not surprisingly, the second reduction of all the complexes exhibited catalysis on proton reduction, Fig. S7. This catalysis supports, on the other hand, the assignment that the second reduction process is the successive reduction from "Fe(I)Fe(0)" to "Fe(0)Fe(0)" of the **EE** mechanism. It must be pointed out that those peak currents increasing with the acid concentration can certainly be assigned to the catalysis by the reduced species of the diiron mimics as revealed by the control (Fig. S8) but exact nature of the catalytic species is unknown.

4. Conclusions

In this piece of work, eight diiron complexes with a naphthalene moiety as the bridging linkage have been synthesised and fully characterised. Their electrochemistry and behaviours of catalysis on proton reduction suggest that, like the analogue (**7**) we reported recently,[30] these complexes adopt two competing mechanisms in their electron transfer, that is, **ECE** and **EE** mechanisms (pathway iii, Scheme 1). Due to the conjugating

effect of the naphthalene moiety which lowers the electron density on the diiron centre and thus stabilises the monoanion after accepting the first electron, the competing mechanisms the two sequential one-electron processes (**EE** mechanism) is dominant. The substituent on the naphthalene does not significantly affect the electrochemistry and catalysis on proton reduction if it does not significantly disturb the conjugation of the naphthalene moiety as does it in the cases of complexes **3a** and **3b**. The involvement of the formyl group in the conjugation of the entire naphthalene skeleton altered significantly the electrochemical and catalytic behaviours of the two complexes.

Our results show also that the diiron complexes possessing the naphthalene moiety exhibited decent tolerance towards chemical manipulation under relatively mild conditions. The tolerance offers possibilities of accessing novel diiron complexes starting from complexes such as **3a** and **3b** to achieve mimics of additional functionalities.

Acknowledgments

We thank the National Natural Science Foundation of China (Grant Nos. 21171073, 20871064), Ministry of Science and Technology (China) (973 program, Grant No: 2009CB220009), and the Government of Zhejiang Province (Qianjiang professorship for XL) for supporting this work.

Notes and references

[a] *College of Biological, Chemical Sciences and Engineering, Jiaxing University, Jiaxing, Zhejiang 314001, China. Tel./Fax: +86(0)573 83643937; E-mail: xiaoming.liu@mail.zjxu.edu.cn.*

[b] *School of Chemistry, Nanchang University, Nanchang, Jiangxi 330031, China.*

† Electronic Supplementary Information (ESI) available: IR and UV/Vis spectra of diiron hexacarbonyl complexes, CVs of **2a** and **2b**, CVs of diiron hexacarbonyl complexes at various scanning rates in DCM, current functions of diiron hexacarbonyl complexes in MeCN and catalytic reduction of proton in MeCN-acetic acid. See DOI: 10.1039/b000000x/

1. J. W. Peters, W. N. Lanzilotta, B. J. Lemon and L. C. Seefeldt, *Science*, 1998, **282**, 1853–1858.
2. Y. Nicolet, C. Piras, P. Legrand, C. E. Hatchikian and J. C. Fontecilla-Camps, *Structure*, 1999, **7**, 13–23.
3. X. M. Liu, S. K. Ibrahim, C. Tard and C. J. Pickett, *Coord. Chem. Rev.*, 2005, **249**, 1641–1652.
4. J. C. Fontecilla-Camps, A. Volbeda, C. Cavazza and Y. Nicolet, *Chem. Rev.*, 2007, **107**, 4273–4303.
5. J. F. Capon, F. Gloaguen, F. Y. Petillon, P. Schollhammer and J. Talarmin, *Coord. Chem. Rev.*, 2009, **253**, 1476–1494.
6. F. Gloaguen and T. B. Rauchfuss, *Chem. Soc. Rev.*, 2009, **38**, 100–108.
7. C. Tard and C. J. Pickett, *Chem. Rev.*, 2009, **109**, 2245–2274.
8. T. R. Simmons, G. Berggren, M. Bacchi, M. Fontecave and V. Artero, *Coord. Chem. Rev.*, 2014, **270–271**, 127–150.
9. N. Wang, M. Wang, Y. Wang, D. Zheng, H. Han, M. S. G. Ahlquist and L. Sun, *J. Am. Chem. Soc.*, 2013, **135**, 13688–13691.
10. T. B. Liu and M. Y. Darensbourg, *J. Am. Chem. Soc.*, 2007, **129**, 7008–7009.
11. A. K. Justice, L. De Gioia, M. J. Nilges, T. B. Rauchfuss, S. R. Wilson and G. Zampella, *Inorg. Chem.*, 2008, **47**, 7405–7414.
12. A. K. Justice, M. J. Nilges, T. B. Rauchfuss, S. R. Wilson, L. De Gioia and G. Zampella, *J. Am. Chem. Soc.*, 2008, **130**, 5293–5301.
13. C. M. Thomas, T. B. Liu, M. B. Hall and M. Y. Darensbourg, *Inorg. Chem.*, 2008, **47**, 7009–7024.
14. M. Karnahl, S. Tschierlei, O. F. Erdem, S. Pullen, M. P. Santoni, E. J. Reijerse, W. Lubitz and S. Ott, *Dalton Trans.*, 2012, **41**, 12468–12477.
15. B. E. Barton, M. T. Olsen and T. B. Rauchfuss, *J. Am. Chem. Soc.*, 2008, **130**, 16834–16835.
16. M. T. Olsen, T. B. Rauchfuss and S. R. Wilson, *J. Am. Chem. Soc.*, 2010, **132**, 17733–17740.
17. O. F. Erdem, L. Schwartz, M. Stein, A. Silakov, S. Kaur-Ghumaan, P. Huang, S. Ott, E. J. Reijerse and W. Lubitz, *Angew. Chem. Int. Ed.*, 2011, **50**, 1439–1443.
18. D. Schilter and T. B. Rauchfuss, *Angew. Chem. Int. Ed.*, 2013, **52**, 13518–13520.
19. G. Berggren, A. Adamska, C. Lambertz, T. R. Simmons, J. Esselborn, M. Atta, S. Gambarelli, J. M. Mouesca, E. Reijerse, W. Lubitz, T. Happe, V. Artero and M. Fontecave, *Nature*, 2013, **499**, 66–69.
20. G. A. N. Felton, C. A. Mebi, B. J. Petro, A. K. Vannucci, D. H. Evans, R. S. Glass and D. L. Lichtenberger, *J. Organomet. Chem.*, 2009, **694**, 2681–2699.
21. X. H. Zeng, Z. M. Li, Z. Y. Xiao, Y. W. Wang and X. M. Liu, *Electrochem. Commun.*, 2010, **12**, 342–345.
22. J. Zhao, Z. H. Wei, X. H. Zeng and X. M. Liu, *Dalton Trans.*, 2012, **41**, 11125–11133.
23. A. J. Bard and L. R. Faulkner, *Electrochemical methods : fundamentals and applications*, 2nd edn., Wiley, New York, 2001.
24. G. A. N. Felton, B. J. Petro, R. S. Glass, D. L. Lichtenberger and D. H. Evans, *J. Am. Chem. Soc.*, 2009, **131**, 11290–11291.
25. A. K. Vannucci, S. H. Wang, G. S. Nichol, D. L. Lichtenberger, D. H. Evans and R. S. Glass, *Dalton Trans.*, 2010, **39**, 3050–3056.
26. G. A. N. Felton, A. K. Vannucci, J. Chen, L. T. Lockett, N. Okumura, B. J. Petro, U. I. Zakai, D. H. Evans, R. S. Glass and D. L. Lichtenberger, *J. Am. Chem. Soc.*, 2007, **129**, 12521–12530.
27. F. Gloaguen, D. Morvan, J. F. Capon, P. Schollhammer and J. Talarmin, *J. Electroanal. Chem.*, 2007, **603**, 15–20.
28. L. Schwartz, P. S. Singh, L. Eriksson, R. Lomoth and S. Ott, *C. R. Chim.*, 2008, **11**, 875–889.
29. D. Streich, M. Karnahl, Y. Astuti, C. W. Cady, L. Hammarstrom, R. Lomoth and S. Ott, *Eur. J. Inorg. Chem.*, 2011, 1106–1111.
30. G. F. Qian, H. L. Wang, W. Zhong and X. M. Liu, *Electrochim. Acta*, 2015, **163**, 190–195.
31. Y. W. Wang, Z. M. Li, X. H. Zeng, X. F. Wang, C. X. Zhan, Y. Q. Liu, X. R. Zeng, Q. Y. Luo and X. M. Liu, *New J. Chem.*, 2009, **33**, 1780–1789.
32. Y. Tang, Z. H. Wei, W. Zhong and X. M. Liu, *Eur. J. Inorg. Chem.*, 2011, 1112–1120.
33. Z. Y. Xiao, Z. H. Wei, L. Long, Y. L. Wang, D. J. Evans and X. M. Liu, *Dalton Trans.*, 2011, **40**, 4291–4299.
34. R. J. Wright, C. Lim and T. D. Tilley, *Chem. Eur. J.*, 2009, **15**, 8518–8525.
35. A. P. S. Samuel, D. T. Co, C. L. Stern and M. R. Wasielewski, *J. Am. Chem. Soc.*, 2010, **132**, 8813–8815.
36. C. Figliola, L. Male, P. N. Horton, M. B. Pitak, S. J. Coles, S. L. Horswell and R. S. Grainger, *Organometallics*, 2014, **33**, 4449–4460.
37. C. Topf, U. Monkowius and G. Knör, *Inorg. Chem. Commun.*, 2012, **21**, 147–150.
38. L. Chen, M. Wang, F. Gloaguen, D. H. Zheng, P. L. Zhang and L. C. Sun, *Chem. Eur. J.*, 2012, **18**, 13968–13973.
39. L. Chen, M. Wang, F. Gloaguen, D. H. Zheng, P. L. Zhang and L. C. Sun, *Inorg. Chem.*, 2013, **52**, 1798–1806.
40. H. Wang, Y. Xie, R. B. King and H. F. Schaefer, *J. Am. Chem. Soc.*, 2006, **128**, 11376–11384.
41. T. Kojima, D. Noguchi, T. Nakayama, Y. Inagaki, Y. Shiota, K. Yoshizawa, K. Ohkubo and S. Fulkuzumi, *Inorg. Chem.*, 2008, **47**, 886–895.
42. E. W. Miller, S. X. Bian and C. J. Chang, *J. Am. Chem. Soc.*, 2007, **129**, 3458–3459.
43. X. H. Zeng, Z. M. Li and X. M. Liu, *Electrochim. Acta*, 2010, **55**, 2179–2185.
44. X. H. Zeng, Z. M. Li, Z. Y. Xiao, Y. W. Wang and X. M. Liu, *Electrochem. Commun.*, 2010, **12**, 342–345.
45. G. M. Sheldrick, *Acta Crystallogr., Sect. A: Found. Crystallogr.*, 2008, **64**, 112–122.

46. M. J. T. Frisch, G. W. Trucks, H. B. Schlegel, G. E. Scuseria, M. A. Robb, J. R. Cheeseman, J. A. Montgomery Jr., T. Vreven, K. N. Kudin, J. C. Burant, J. M. Millam, S. S. Iyengar, J. Tomasi, V. Barone, B. Mennucci, M. Cossi, G. Scalmani, N. Rega, G. A. Petersson, H. Nakatsuji, M. Hada, M. Ehara, K. Toyota, R. Fukuda, J. Hasegawa, M. Ishida, T. Nakajima, Y. Honda, O. Kitao, H. Nakai, M. Klene, X. Li, J. E. Knox, H. P. Hratchian, J. B. Cross, V. Bakken, C. Adamo, J. Jaramillo, R. Gomperts, R. E. Stratmann, O. Yazyev, A. J. Austin, R. Cammi, C. Pomelli, J. W. Ochterski, P. Y. Ayala, K. Morokuma, G. A. Voth, P. Salvador, J. J. Dannenberg, V. G. Zakrzewski, S. Dapprich, A. D. Daniels, M. C. Strain, O. Farkas, D. K. Malick, A. D. Rabuck, K. Raghavachari, J. B. Foresman, J. V. Ortiz, Q. Cui, A. G. Baboul, S. Clifford, J. Cioslowski, B. B. Stefanov, G. Liu, A. Liashenko, P. Piskorz, I. Komaromi, R. L. Martin, D. J. Fox, T. Keith, M. A. Al-Laham, C. Y. Peng, A. Nanayakkara, M. Challacombe, P. M. W. Gill, B. Johnson, W. Chen, M. W. Wong, C. Gonzalez and J. A. Pople, *GAUSSIAN 03 (Revision E.01)*, 2003.

47. J. P. Perdew, *Phys. Rev. B*, 1986, **33**, 8822–8824.

48. A. D. Becke, *Phys. Rev. A*, 1988, **38**, 3098–3100.

49. F. Weigend and R. Ahlrichs, *Phys. Chem. Chem. Phys.*, 2005, **7**, 3297–3305.

50. A. J. Ashe, J. W. Kampf and P. M. Savla, *Heteroatom Chem.*, 1994, **5**, 113–119.

51. P. Li, S. Amirjalayer, F. Hartl, M. Lutz, B. d. Bruin, R. Becker, S. Woutersen and J. N. H. Reek, *Inorg. Chem.*, 2014, **53**, 5373–5383.

52. H. L. Wang and X. M. Liu, *Inorg. Chim. Acta*, 2013, **406**, 113–118.

Table 2 Crystallographic data for complexes **3a**, **3b**, **4b**, **5b**, **6a** and **7**.

Complex	**3a**	**3b**	**4b**	**5b**	**6a**	**7**
Chemical formula	$C_{17}H_6O_7S_2Fe_2$	$C_{17}H_6O_7S_2Fe_2$	$C_{17}H_8O_7S_2Fe_2$	$C_{21}H_{13}O_8S_2Fe_2Cl$	$C_{21}H_{13}O_8S_2Fe_2Br$	$C_{29}H_{18}O_8S_2Fe_3Cl_2$
F_w	498.04	498.04	500.05	604.58	649.04	797.00
Temp. (K)	296(2)	296(2)	296(2)	296(2)	296(2)	296(2)
Radiation	0.71073	0.71073	0.71073	0.71073	0.71073	0.71073
Crystal system	Triclinic	Triclinic	Triclinic	Monoclinic	Triclinic	Triclinic
Space group	P-1	P-1	P-1	P2(1)	P-1	P-1
a/Å	7.556(5)	7.9316(11)	8.0499(10)	7.9363(12)	7.710(3)	7.653(8)
b/Å	9.504(7)	8.4597(12)	8.5617(11)	34.734(5)	11.306(4)	14.654(15)
c/Å	14.246(10)	14.947(2)	14.8223(18)	17.444(3)	15.523(5)	14.902(15)
α / (°)	86.686(8)	90.946(2)	91.110(2)	90.00	110.397(4)	68.932(11)
β / (°)	79.551(8)	101.791(2)	102.7310(10)	94.006(2)	91.963(4)	78.682(11)
γ / (°)	66.911(8)	109.5740(10)	109.1460(10)	90.00	107.447(4)	84.567(12)
V, Å^3	925.4(11)	921.1(2)	936.7(2)	4796.9(13)	1195.2(7)	1529(3)
Z	2	2	2	8	2	2
D_c / (g/cm^{-3})	1.787	1.796	1.773	1.674	1.803	1.732
θ range (deg)	2.33 to 25.00	2.57 to 26.00	2.53 to 25.00	2.41 to 25.00	2.80 to 25.00	2.45 to 25.00
F(000)	496	496	500	2432	644	800
Reflections collected(R_{int})	6692 (0.0182)	7326 (0.0186)	6783 (0.0187)	35686 (0.0190)	5828 (0.0202)	7337 (0.0163)
Reflections independent	3233	3569	3288	15924	3784	4989
GOF	1.002	1.037	1.026	1.045	1.037	1.022
$R_1[I > 2\sigma(I)]$	0.0263	0.0342	0.0308	0.0360	0.0485	0.0373
wR_2 (all data)	0.0725	0.1059	0.0909	0.0911	0.1402	0.1029

Table 3 Selected bonding parameters of the complexes **3a**, **3b**, **4b**, **5b**, **6a** and **7**.

Complexes	**3a**	**3b**	**4b**	**5b**	**6a**	**7**
Fe(1)-Fe(2)	2.5169(18)	2.5100(7)	2.5140(6)	2.5270(10)	2.5108(12)	2.509(2)
Fe(1)-S(1)	2.2382(15)	2.2509(10)	2.2532(8)	2.2482(14)	2.2466(15)	2.241(2)
Fe(1)-S(2)	2.2371(13)	2.2422(9)	2.2427(8)	2.2403(14)	2.2399(14)	2.241(2)
Fe(2)-S(1)	2.2414(12)	2.2444(10)	2.2476(8)	2.2499(14)	2.2444(15)	2.239(2)
Fe(2)-S(2)	2.2393(14)	2.2436(9)	2.2455(8)	2.2408(15)	2.2406(15)	2.2405(18)
S(1)-C(7)	1.772(2)	1.783(3)	1.783(3)	1.766(5)	1.784(5)	1.772(4)
S(2)-C(15)	1.778(2)	1.771(3)	1.770(3)	1.738(5)	1.771(4)	1.775(3)
S(1)-Fe(1)-Fe(2)	55.88(2)	55.93(3)	55.94(2)	55.85(4)	55.97(4)	55.90(7)
S(2)-Fe(1)-Fe(2)	55.83(4)	56.00(3)	55.99(2)	55.68(4)	55.93(4)	55.95(3)

Fe(1)-S(1)-Fe(2)	68.37(6)	67.88(3)	67.92(2)	68.36(4)	67.98(5)	68.11(5)
Fe(1)-S(2)-Fe(2)	68.42(5)	68.05(3)	68.13(2)	68.65(4)	68.17(4)	68.08(6)
S(1)-Fe(2)-Fe(1)	55.76(5)	56.18(3)	56.15(2)	55.79(4)	56.05(4)	55.99(4)
S(2)-Fe(2)-Fe(1)	55.75(2)	55.95(3)	55.88(2)	55.66(4)	55.90(4)	55.97(7)
S(1)-Fe(1)-S(2)	84.02(4)	84.14(3)	84.17(3)	84.22(5)	84.28(5)	84.02(4)
S(1)-Fe(2)-S(2)	83.89(4)	84.26(3)	84.23(3)	84.17(5)	84.31(5)	84.09(5)

Table 4 Electrochemical data for the diiron complexes and compounds **2a** and **2b**.[a]

	DCM			MeCN		
	Reduction ($^aE_1$ / $^cE_1$, $^cE_2$)	$^cE_1$–$^cE_2$	Oxidation (^aE)	Reduction ($^aE_1$ / $^cE_1$, $^cE_2$)	$^cE_1$–$^cE_2$	Oxidation (^aE)
3a	–1.44 / –1.51[b] (–1.48)	< 30	0.86	–1.36 / –1.46 (–1.41), –1.60	140	0.75
[c]**3a**				–1.28 / –1.36 (–1.32), –1.63	270	
3b	–1.46 / –1.54[b] (–1.50)	< 30	0.69	–1.37 / –1.45 (–1.41), –1.55	100	0.77
[c]**3b**				–1.29 / –1.37 (–1.33), –1.58	210	
4a	–1.52 / –1.62 (–1.57), –1.88	260	0.82	–1.44 / –1.53 (–1.49), –1.88	350	0.79
4b	–1.54 / –1.65 (–1.60), –1.87	220	0.82	–1.46 / –1.54 (–1.50), –1.87	330	0.81
5a	–1.52 / –1.60 (–1.56), –1.93	330	0.89	–1.43 / –1.51 (–1.47), –1.87	360	0.85
5b	–1.53 / –1.63 (–1.58), –1.95	320	0.90	–1.44 / –1.51 (–1.48), –1.89	380	0.84
6a	–1.52 / –1.61 (–1.57), –1.93	320	0.90	–1.44 / –1.51 (–1.48), –1.88	370	0.82
6b	–1.54 / –1.63 (–1.59), –1.96	330	0.89	–1.44 / –1.51 (–1.48), –1.90	390	0.82
7	–1.53 / –1.62 (–1.58), –1.92	300	[d]0.85			
8	–1.52 / –1.61 (–1.57), –1.92	310	0.94	–1.44 / –1.52 (–1.48), –1.91	390	
2a				–1.66, –1.79	130	0.70
2b	–1.52, –1.98	460	0.69			

[a] $E_{1/2}$ is placed in a parenthesis where applicable.
[b] The second reduction peak potential $^cE_2$ overlaps with $^cE_1$.
[c] The data were collected in DMF.
[d] $E_{1/2}$ of the pendant ferrocenyl group is 0.27 V.[30]

Graphic abstract

Diiron hexacarbonyl complexes bearing naphthalene-1,8-dithiolate moiety bridge as the mimics of the sub-unit of [FeFe]-hydrogenase: Synthesis, characterisation and electrochemical investigations

Guifen Qian,[b] Wei Zhong,[a] Zhenhong Wei,[b] Hailong Wang,[a] Zhiyin Xiao,[a] Li Long[a] and Xiaoming Liu*[,a, b]

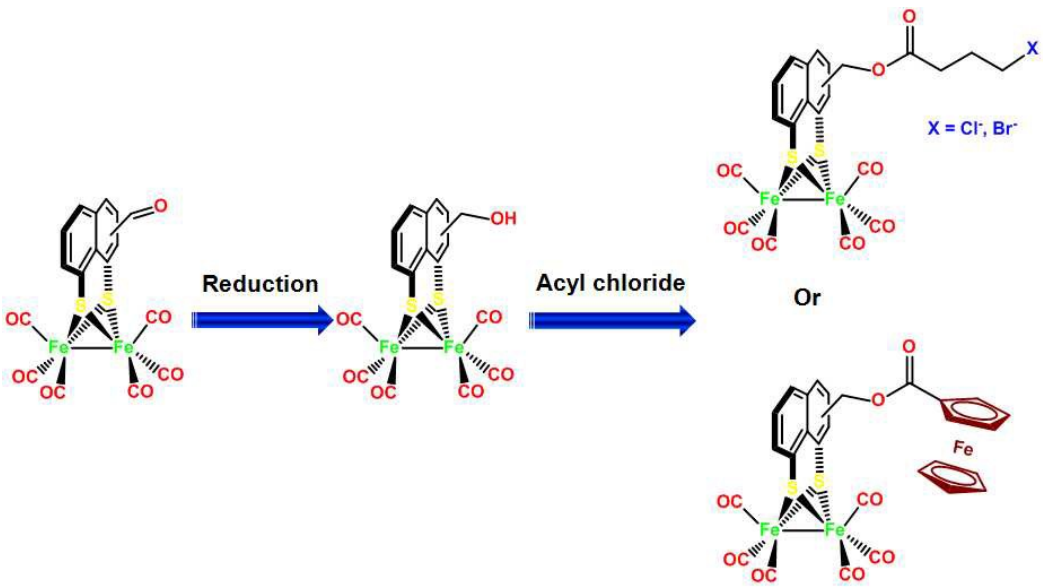

Reducing the formyl group into a hydroxyl group allows the further synthesis of novel diiron complexes with various functionalities.